Inorg. Chem. **2009**, *48*, 4052−4061

Establishing Amide···Amide Reliability and Synthon Transferability in the Supramolecular Assembly of Metal-Containing One-Dimensional Architectures

Christer B. Aakeröy,* Benjamin M. T. Scott, Michelle M. Smith, Joaquin F. Urbina, and John Desper

Department of Chemistry, Kansas State University, CBC Hall, Manhattan, Kansas 66506

Received October 17, 2008

On the basis of a combination of new structural data (eleven single-crystal structure determinations are presented) and information from the Cambridge Structural Database, it has been shown that self-complementary hydrogen-bond based amide···amide dimers can be relied upon as effective supramolecular synthons for the assembly and organization of *acac*- and paddle-wheel complexes of a variety of metal(II) ions. The targeted molecular recognition event and intended extended one-dimensional motif appear with a supramolecular yield of 78% (a total of 28 structures were examined). Despite the fact that the hydrogen bonds that give rise to the $R_2^2(8)$ motif can be disrupted by both carboxylate- and *acac*-ligands, as well as by solvent molecules, they remain remarkably resilient and therefore represent useful synthetic tools in inorganic crystal engineering.

Introduction

The construction of metal-containing supramolecular architectures has proceeded primarily through ligand−metal interactions producing "coordination polymers",[1] or via a combination of metal−ligand and non-covalent ligand−ligand interactions.[2] The former approach has led to the publication of over 4000 papers in the last five-year period, and this field continues to expand unabated.[1] Strategies that employ coordinate-covalent bonds coupled with the deliberate use of directional hydrogen bonds, on the other hand, have not received anywhere near the same attention. Nevertheless, materials that are constructed with inherently weaker bonds may display better solubility and greater structural flexibility when compared to their coordination-polymer counterparts because of the relative elasticity of non-covalent interactions. However, any synthetic protocol that relies on hydrogen bonds is also likely to be less reliable because of the potential structural interference that solvent molecules and counterions offer. Furthermore, even though the metal ions themselves are frequently a source of desirable properties (e.g., magnetism,[3] catalysis[4]), or structure-driving capability (e.g., as nodes in three-dimensional porous networks[5]), many transition-metal ions are capable of displaying a range of coordination numbers/geometries which often ruins attempts at "controlled" assembly. Consequently, a major challenge

* To whom correspondence should be addressed. E-mail: aakeroy@ksu.edu.

(1) (a) Duriska, M. B.; Batten, S. R.; Price, D. J. *Aus. J. Chem.* **2006**, *59*, 26. (b) Du., M.; Zhao, X.-J.; Batten, S. R.; Ribas, J. *Cryst. Growth. Des.* **2005**, *5*, 901. (c) Matsuda, R.; Kitaura, R.; Kitigawa, S.; Kubota, Y.; Kobayashi, T. C.; Horike, S.; Takata, M. *J. Am. Chem. Soc.* **2004**, *126*, 14063. (d) Bu, X.-H.; Tong, M.-L.; Chang, H.-C.; Kitigawa, S.; Batten, S. *Angew. Chem., Int. Ed.* **2003**, *43*, 192. (e) Abrahams, B. F.; Batten, S. R.; Hoskins, B. F.; Robson, R. *Inorg. Chem.* **2003**, *42*, 2654. (f) Maji, T. K.; Kitigawa, S. *Pure Appl. Chem.* **2007**, *79*, 2150. (g) Cordes, D. B.; Sharma, C. V. K.; Rogers, R. *Cryst. Growth Des.* **2007**, *7*, 1943. (h) Robson, R. *J. Chem. Soc., Dalton Trans.* **2000**, 3735.

(2) (a) Aakeröy, C. B.; Schultheiss, N.; Desper, J. *Dalton. Trans.* **2006**, 1627. (b) Aakeröy, C. B.; Schultheiss, N.; Desper, J. *CrystEngComm* **2006**, *9*, 421. (c) Aakeröy, C. B.; Schultheiss, N.; Desper, J. *Inorg. Chem.* **2005**, *44*, 4983. (d) Aakeröy, C. B.; Desper, J.; Martínez, J. V. *CrystEngComm* **2004**, *6*, 413. (e) Aakeröy, C. B.; Beatty, A. M.; Lorimer, K. R. *J. Chem. Soc., Dalton Trans.* **2000**, 3869. (f) Aakeröy, C. B.; Beatty, A. M.; Leinen, D. S.; Lorimer, K. R. *Chem. Commun.* **2000**, 935. (g) Burchell, T. J.; Eisler, D. J.; Puddephatt, R. J. *Inorg. Chem.* **2004**, *43*, 5550. (h) Stephenson, M. D.; Prior, T. J.; Hardie, M. J. *Cryst. Growth Des.* **2008**, *8*, 643. (i) Brammer, L. *Chem. Soc. Rev.* **2004**, *33*, 476, and references therein. (j) Hofmeier, H.; El-ghayoury, A.; Schenning, A. P. H. J.; Schubert, U. S. *Chem. Commun.* **2004**, 318. (k) Kruth, D. J.; Fromm, K. M.; Lehn, J.-M. *Eur. J. Inorg. Chem.* **2001**, 1523. (l) Breuning, E.; Ziener, U.; Lehn, J.-M.; Wegelius, E.; Rissanen, K. *Eur. J. Inorg. Chem.* **2001**, 1515. (m) Schauer, C. L.; Matwey, E.; Fowler, F. W.; Lauher, J. W. *J. Am. Chem. Soc.* **1997**, *119*, 10245. (n) Deiters, E.; Bulach, V.; Hosseini, M. W. *New J. Chem.* **2008**, *32*, 99. (o) Burchell, T. J.; Eisler, D. J.; Puddephatt, R. J. *Chem. Commun.* **2004**, 944. (p) Yue, N. L. S.; Eisler, D. J.; Jennings, M. C.; Puddephatt, R. *Inorg. Chem.* **2004**, *43*, 7671. (q) Pansanel, J.; Jouaiti, A.; Ferlay, S.; Hosseini, M. W.; Planeix, J.-M.; Kyritsakas, N. *New. J. Chem.* **2006**, *30*, 71. (r) Natale, D.; Mareque-Rivas, C. *Chem. Commun.* **2008**, 425. (s) Martínez-Vargas, S.; Hernández-Ortega, S.; Toscano, R. A.; Salazar-Mendoza, D.; Valdés-Martínez, J. *CrystEngComm.* **2008**, *10*, 86.

10.1021/ic801992t CCC: $40.75
Published on Web 04/02/2009

in crystal engineering is presented by the lack of reliable and versatile synthetic methods for preparing coordination networks with specific topologies and dimensionalities.

The assembly and spatial organization of a series of coordination complexes could, in principle, be accomplished using a bifunctional ligand, where one end of the ligand binds to a metal ion, whereas the second moiety is capable of forming a structure-directing interaction with a neighboring ligand through a well-defined and preconceived supramolecular synthon.[6] Ideally, the metal−ligand and ligand−ligand interactions should be insensitive to the relative positioning of the two binding sites on the ligand, and the shape/size of the coordination complex should not affect the desired molecular-recognition events. The nature of the resulting extended network (e.g., dimensionality, topology, and metrics) could then be varied/controlled in a systematic manner through simple covalent modifications of the ligand.

The goal of this study is to establish the robustness of a supramolecular synthetic strategy based upon a ligand comprising an N-heterocycle (for binding to the metal ion) and an amide (for providing intermolecular amide···amide synthons).

To determine the ability of such ligands to achieve the desired metal-containing extended structural motif in the absence of potentially disruptive counterions, we decided to target a set of neutral coordination complexes, Scheme 1. In addition, by using chelating ligands we also restrict the number of possible geometries that each metal ion can adopt, thereby simplifying the assembly process further.

Scheme 1. Equatorially "Blocked" (a) *acac* Complex and (b) "paddle-wheel" Complex with Axial Sites (Arrows) Available for Coordination by Two Additional Ligands

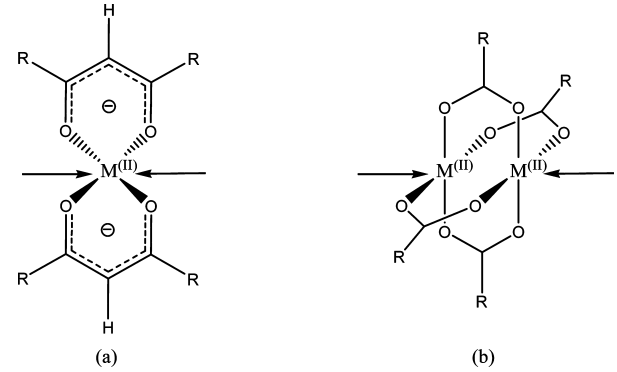

Scheme 2. Representation of the Targeted Supramolecular 1-D Chain Constructed via Both Metal Coordination (Shown As a Circle), and Amide···Amide Hydrogen-Bonding

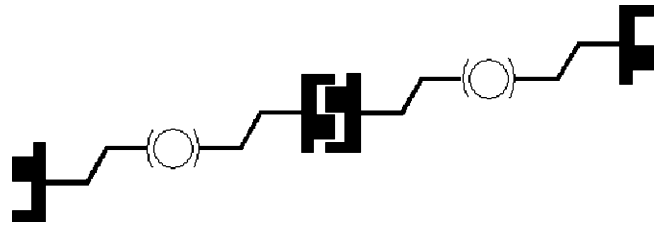

The supramolecular target in each case presented in this study is first of all an infinite one-dimensional (1-D) chain, Scheme 2. Therefore, each metal complex is required to have exactly two available binding sites that can be occupied by N-heterocycle/amide ligands.

Bidentate acetylacetonate (*acac*) and acetate "paddle-wheel" complexes are particularly useful in this context as they both produce neutral complexes (with M^{2+} metal ions) that present two open binding sites oriented in a *trans*-geometry, Scheme 1.[7]

Isonicotinamide[8] and benzimidazol-1-yl benzamides[9] have previously been used successfully to create infinite 1-D chains with Ag(I), and the former has also been employed extensively with more complex ions.[10] However, there have been no systematic studies of the relative effectiveness of a series of N-heterocycle/amide ligands to connect neutral coordination complexes into infinite 1-D chains. We now present the structural outcome of reactions between six different N-heterocycle/amide ligands, Scheme 3, and a series of *acac* and paddle-wheel based complexes. This will allow us to establish whether or not the assembly process is sensitive to how the N-heterocycle/amide ligand is con-

(3) (a) Gao, D.-Z.; Liao, D.-L.; Jiang, Z.-H.; Yan, S.-P. *Transition Met. Chem.* **2008**, *33*, 107. (b) Wang, X.-Y.; Wang, Z.-M.; Gao, S. *Chem. Commun.* **2008**, 281. (c) Ju, Z.-F.; Yao, Q.-X.; Wu, W.; Zhang, J. *Dalton Trans.* **2008**, 355. (d) Selvan, R. K.; Krishnan, V.; Augustin, C. O.; Bertagnolli, H.; Kim, C. S.; Gedanken, A. *Chem. Mater.* **2008**, *20*, 429. (e) Pardo, E.; Carrasco, R.; Ruiz-Garcia, R.; Julve, M.; Lloret, F.; Munoz, M. C.; Journaux, Y.; Ruiz, E.; Cano, J. *J. Am. Chem. Soc.* **2008**, *130*, 576. (f) Tuncel, M.; Oezbuelbuel, A.; Serin, S. *React. Funct. Polym.* **2008**, *68*, 292. (g) Parent, A. R.; Vedachalam, S.; Landee, C. P.; Turnbull, M. M. *J. Coord. Chem.* **2008**, *61*, 93. (h) Roques, N.; Maspoch, D.; Luis, F.; Camon, A.; Wurst, K.; Datcu, A.; Rovira, C.; Ruiz-Molina, D.; Veciana, J. *J. Mater. Chem.* **2007**, *18*, 98. (i) Costes, J.-P.; Gheorghe, R.; Andruh, M.; Shova, S.; Clemente Juan, J.-M. *New J. Chem.* **2006**, *30*, 572. (j) Atakol, O.; Boca, R.; Ercan, I.; Ercan, F.; Fuess, H.; Haase, W.; Herchel, R. *Chem. Phys. Lett.* **2006**, *423*, 192.

(4) (a) Greatti, A.; Scarpellini, M.; Peralta, R. A.; Casellato, A.; Bortoluzzi, A. J.; Xavier, F. R.; Jovito, R.; Aires de Brito, M.; Szpoganicz, B.; Tomkowicz, Z.; Rams, M.; Haase, W.; Neves, A. *Inorg. Chem.* **2008**, *47*, 1107. (b) Jenkins, W. T.; Patrick, J. S. *J. Inorg. Biochem.* **1986**, *27*, 163. (c) Zalatan, J. G.; Catrina, I.; Mitchell, R.; Grzyska, P. K.; O′Brien, P. J.; Herschlag, D.; Hengge, A.; Alvan, C. *J. Am. Chem. Soc.* **2007**, *129*, 9789. (d) Gantt, S. L.; Gattis, G.; Fierke, C. A. *Biochem.* **2006**, *45*, 6170. (e) Hou, Y.-M.; Gu, S.-Q.; Zhou, H.; Ingerman, L. *Biochem.* **2005**, *44*, 12849.

(5) (a) Du, M.; Jiang, X.-J.; Zhao, X.-J. *Inorg. Chem.* **2007**, *46*, 3984. (b) Yaghi, O. M.; Li, H.; Davis, C.; Richardson, D.; Groy, T. L. *Acc. Chem. Res.* **1998**, *31*, 474. (c) Kawano, M.; Kawamichi, T.; Haneda, T.; Kojima, T.; Fujita, M. *J. Am. Chem. Soc.* **2007**, *129*, 15418. (d) Takaoka, K.; Kawano, M.; Hozumi, T.; Ohkoshi, S.-I.; Fujita, M. *Inorg. Chem.* **2006**, *45*, 3976. (e) Fujita, M.; Yazaki, J.; Ogura, K. *J. Am. Chem. Soc.* **1990**, *112*, 5645. (f) Fujita, M.; Oguro, D.; Miyazawa, M.; Oka, H.; Yamaguchi, K.; Ogura, K. *Nature (London)* **1995**, *378*, 469. (g) Hawxwell, S. M.; Espallargas, G. M.; Bradshaw, D.; Rosseinsky, M. J.; Timothy, J.; Florence, A. J.; van de Streek, J.; Brammer, L. *Chem. Commun.* **2007**, 1532. (h) Li, H.; Eddaoudi, M.; Groy, T. L.; Yaghi, O. M. *J. Am. Chem. Soc.* **1998**, *120*, 8571. (i) Sudik, A. C.; Millward, A. R.; Ockwig, N. W.; Côté, A. P.; Kim, J.; Yaghi, O. M. *J. Am. Chem. Soc.* **2005**, *127*, 7110.

(6) (a) Desiraju, G. R. *Angew. Chem., Int. Ed. Engl.* **1995**, *34*, 2311. (b) Desiraju, G. *Crystal Engineering-The Design of Organic Solids*; Elsevier: Amsterdam, 1989.

(7) (a) Pansanel, J.; Jouaiti, A.; Ferlay, S.; Hosseini, M. W.; Planeix, J.-M.; Kyritsakas, N. *New. J. Chem.* **2006**, *30*, 683. (b) Dikarev, E. V.; Gray, T. G.; Li, B. *Angew. Chem., Int. Ed.* **2005**, *44*, 1721. (c) Cotton, F. A.; Jin, J.-Y.; Li, Z.; Liu, C. Y.; Murillo, C. A. *Dalton Trans.* **2007**, 2328. (d) Pan, L.; Olson, D. H.; Ciemnolonski, L. R.; Heddy, R.; Li, J. *Angew. Chem., Int. Ed.* **2006**, *45*, 616. (e) Barrios, L. A.; Ribas, J.; Aromi, G.; Ribas-Arino, J.; Gamez, P.; Roubeau, O.; Teat, S. J. *Inorg. Chem.* **2007**, *46*, 7154. (f) Soldatov, D. V.; Ripmeester, J. A. *Chem.—Eur. J.* **2001**, *7*, 2979. (g) Hearns, N. G. R.; Hesp, K. D.; Jennings, M.; Jasmine, J. L.; Preuss, K. E. *Polyhedron* **2007**, *26*, 2047.

(8) (a) Aakeröy, C. B.; Beatty, A. *Cryst. Eng.* **1998**, *1*, 39. (b) Aakeröy, C. B.; Beatty, A. *Chem. Commun.* **1998**, 1067.

(9) Aakeröy, C. B.; Desper, J.; Smith, M. M.; Urbina, J. F. *Dalton Trans.* **2005**, 2462.

Scheme 3. Bifunctional Ligands: 4-[(2-Methylbenzimidazol-1-yl)methyl]-benzamide **1**, 4-[(5,6-Dimethylbenzimidazol-1-yl)methyl]-benzamide **2**, 4-[2-Phenylimidazol-1-yl)methyl]-benzamide **3**, 3-[2-Phenylimidazol-1-yl)methyl]-benzamide **4**, 4-[Pyrazol-1-yl)methyl]-benzamide **5**, 3-[Pyrazol-1-yl)methyl]-benzamide **6**

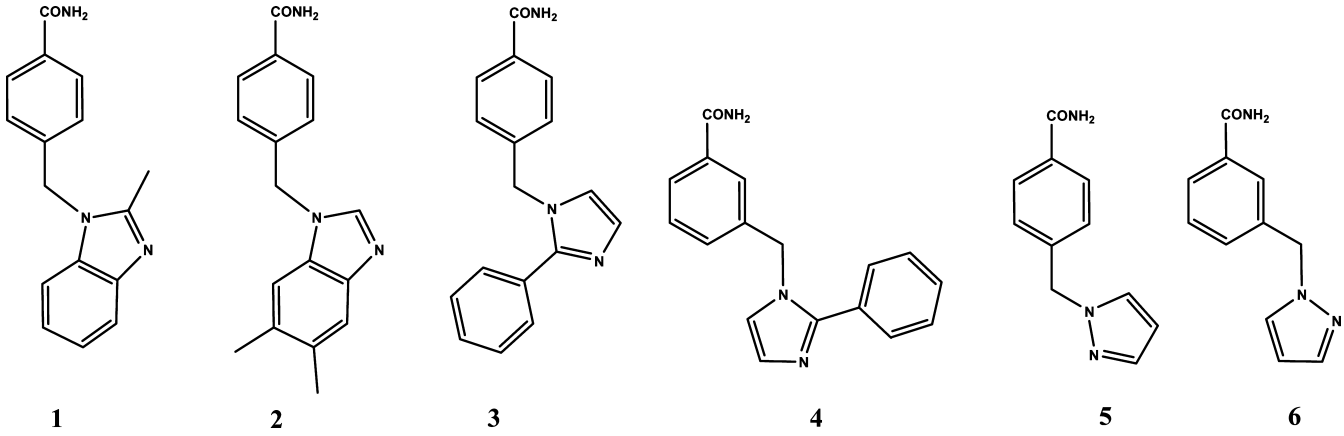

structed and, therefore, if the synthetic process itself is likely to be versatile and transferable to other targets.

Experimental Section

Materials and Measurements. All chemicals were purchased from Aldrich and used without further purification. Melting points were determined on a Fisher-Johns melting point apparatus and were uncorrected. ^{1}H NMR spectra were recorded on a Varian Unity plus 400 MHz spectrometer (NMR solvent detailed in experimental). Synthesis and characterization of **1**,[11] **2**,[9] **5**, and **6**[12] have been reported elsewhere.

Synthesis.[13] **Synthesis of 4-[(2-Phenylimidazol-1-yl)methyl]benzonitrile.** 2-Phenylimidazole (3.061 g, 21mmol) was dissolved in dry THF (THF, 40 mL) with stirring in a 250 mL round-bottomed flask. To the colorless solution was added NaOH (8.4 g, 210mmol) resulting in an orange solution, which was stirred for 2 h at room temperature under an N_2 atmosphere. To this mixture was added a solution of dry THF (60 mL) containing α-bromo-*p*-tolunitrile (4.12 g, 21.03mmol). Stirring was continued for 24 h under an N_2 atmosphere, after which distilled water (20 mL) was added to dissolve remaining NaOH pellets and the NaBr. The two layers formed were separated using a separatory funnel, and the THF layer was dried over anhydrous $MgSO_4$. The $MgSO_4$ was filtered off, and the solvent removed under vacuum to give a yellow solid (5.26 g, 96%); Mp: 128−130 °C. ^{1}H NMR (δ_H; 400 MHz, $CDCl_3$): 5.30 (s, 2H), 6.98 (d, 1H, J = 4 Hz), 7.16 (d, 2H, J = 8 Hz), 7.24 (d, 1H, J = 4 Hz), 7.40−7.41 (m, 3H), 7.47−7.49 (m, 2H), 7.65 (d, 2H, J = 8 Hz); IR (KBr): 2231 cm^{-1}.

Synthesis of 4-[(2-Phenylimidazol-1-yl)methyl]benzamide, 3. 4-[(2-Phenylimidazol-1-yl)methyl]-benzonitrile (5.2 g, 20.08 mmol) was dissolved in DMSO (30 mL) with heat and stirring in a 250 mL three-necked flask under a N_2 atmosphere. The reaction flask was then cooled in an ice−water bath, and anhydrous K_2CO_3 (0.80 g, 5.77mmol) was added to the reaction mixture. A 30 wt % H_2O_2 solution (60 mL) was added dropwise into the reaction mixture, and a white solid formed almost immediately. The reaction was then allowed to warm to room temperature with continued stirring for 1 h while covered in aluminum foil. Distilled water (50 mL) was added to the reaction mixture. A white solid was obtained upon vacuum filtration, which was washed with two small portions of distilled water and dried (5.06 g, 90%); Mp: 75−80 °C. ^{1}H NMR (δ_H; 400 MHz, $CDCl_3$): 5.28 (s, 2H), 5.83 (bs, 1H), 6.33 (bs, 1H), 6.99 (d, 1H, J = 4 Hz), 7.14 (d, 2H, J = 8 Hz), 7.22 (d, 1H, J = 4 Hz), 7.38−7.40 (m, 3H), 7.49−7.52 (m, 2H), 7.80 (d, 2H, J = 4 Hz); ^{13}C NMR: (δ_C; 400 MHz, $CDCl_3$): 49.99, 121.23, 126.54, 128.15, 128.65, 128.68, 129.06, 129.09, 130.09, 133.04, 140.94, 148.29, 168.74; IR (KBr): 3293, 3179, 1649 cm^{-1}.

Synthesis of 3-[(2-Phenylimidazol-1-yl)methyl]benzonitrile. 2-Phenylimidazole (3.016 g, 20.9 mmol) was dissolved in dry THF (50 mL) with stirring in a 250 mL round-bottomed flask. To the colorless solution was added NaOH (8.36 g, 209mmol), and the mixture was stirred for 2 h at room temperature under an N_2 atmosphere. To this mixture was added a solution of dry THF (60 mL) containing α-bromo-*m*-tolunitrile (4.10 g, 20.91mmol). Stirring was continued for 24 h under a N_2 atmosphere, after which distilled water (10 mL) was added to dissolve the NaOH pellets and NaBr. The two layers formed were separated using a separatory funnel, and the THF layer was dried over anhydrous $MgSO_4$. The $MgSO_4$ was filtered off, and the solvent removed under vacuum to give a yellow oil. Purification by column chromatography (hexanes/ethyl acetate 10:1→4:1) yielded an orange oil (3.52 g, 65%). ^{1}H NMR (δ_H; 400 MHz, $CDCl_3$): 5.18 (s, 2H), 6.92 (1H, d, J = 4 Hz), 7.13 (1H, d, J = 4 Hz), 7.19 (1H, d, J = 8 Hz), 7.24 (1H, s), 7.30 (3H,

(10) (a) Aakeröy, C. B.; Desper, J.; Valdes-Martinez, J. *CrystEngComm.* **2004**, *6*, 413. (b) Bera, J. K.; Vo, T.-T.; Walton, R. A.; Dunbar, K. R. *Polyhedra* **2003**, *22*, 3009. (c) Aakeröy, C. B.; Beatty, A.; Desper, J.; O′Shea, M.; Valdes-Martinez, J. *Dalton Trans.* **2003**, 3956. (d) Zhang, J.-P.; Lin, Y.-Y.; Huang, X.-C.; Chen, X.-M. *J. Am. Chem. Soc.* **2005**, *127*, 5495. (di) Zhang, J.-P.; Lin, Y.-Y.; Huang, X.-C.; Chen, X.-M. *J. Am. Chem. Soc.* **2005**, *127*, 5495. (e) Kozlevcar, B.; Leban, I.; Turel, I.; Segedin, P.; Petric, M.; Pohleven, F.; White, A. J. P.; Williams, D. J.; Sieler, J. *Polyhedra* **1999**, *18*, 755. (f) Tsintsadze, G. V.; Kiguradze, R. A.; Shnulin, A. N.; Mamedov, Kh. S. *Zh. Strukt. Khim.* **1984**, *25*, 82. (g) Smolander, K.; Macko, M.; Valko, M.; Melnik, M. *Anal. Sci. X-Ray Struct. Anal. Online* **2005**, *21*, x167. (h) Chakrabarty, D.; Nagase, H.; Kamijo, M.; Endo, T.; Ueda, H. *Anal. Chem. Scand.* **1992**, *46*, 29. (i) Antsyshkina, A. S.; Koksharova, T. V.; Sadikov, G. G.; Gritsenko, I. S.; Sergienko, V. S.; Egorova, O. A. *Zu. Neorg. Khim.* **2006**, *51*, 972. (j) Kozlevcar, B.; Lah, N.; Leban, I.; Turel, I.; Segedin, P.; Petric, M.; Pohleven, F.; White, A. J. P.; Williams, D. J.; Giester, G. *Croat. Chem. Acta.* **1999**, *72*, 42.

(11) Aakeröy, C. B.; Desper, J.; Urbina, J. *Cryst. Growth Des.* **2005**, *5*, 12183.

(12) Aakeröy, C. B.; Scott, B. M. T.; Desper, J. *New J. Chem.* **2007**, *31*, 2044.

(13) The synthetic methods typically lead to very small amounts of products (the first crystals of suitable size are harvested), and their uniform morphology and color, sharp melting points indicate a structurally homogenous product. The amounts obtained were not enough to allow us to perform X-ray powder diffraction analysis, but for several compounds we determined the unit cell on multiple crystals and they were consistent with the structures reported herein.

m), 7.38 (1H, t, $J = 8$ Hz), 7.39−7.42 (2H, m), 7.48 (1H, d, $J = 8$ Hz); IR (KBr): 2224.10 cm^{-1}.

Synthesis of 3-[(2-Phenylimidazol)methyl]benzamide, 4. 3-[(2-Phenylimidazol-1-yl)methyl]-benzonitrile (3.52 g, 13.6mmol) was dissolved in DMSO (20 mL) with heat and stirring in a 250 mL three-necked flask under a N_2 atmosphere. The reaction flask was then cooled in an ice−water bath, and anhydrous K_2CO_3 (0.57 g, 4.1mmol) was added to the reaction mixture. Thirty wt % H_2O_2 solution (40 mL) was added dropwise into the reaction mixture, and a white solid formed almost immediately. The reaction was then allowed to warm to room temperature with continued stirring for 1 h while covered in aluminum foil. Distilled water (50 mL) was added to the reaction mixture. A solid was obtained upon vacuum filtration, which was washed with two small portions of distilled water and dried. Recrystallization from ethanol gave a white solid (3.34 g, 88%); Mp: 170−174 °C. ^{1}H NMR (δ_H; 400 MHz, $CDCl_3$): 5.27 (s, 2H), 5.81 (bs, 1H), 6.25 (bs, 1H), 6.98 (d, 1H, $J = 4$ Hz), 7.19 (s, 1H), 7.21 (s, 1H), 7.39−7.41 (m, 3H), 7.43 (t, 1H, $J = 4$ Hz), 7.51−7.58 (m, 2H), 7.59 (s, 1H), 7.74 (d, 1H, $J = 8$ Hz);^{13}C NMR: (δ_C, 200 MHz, $CDCl_3$): 50.03, 121.13, 125.75, 126.79, 128.64, 128.73, 128.97, 129.24, 129.35, 129.99, 130.31, 134.10, 137.65, 168.62; IR (KBr): 3324, 3180, 1675 cm^{-1}.

[4-(2-Methylbenzimidazol-1-yl)methylbenzamide]bis-(dibenzoylmethanato)cobalt(II) THF, 1a. 1 (0.040 g, 0.153 mmol) was dissolved in dry THF with heat in a small vial and cooled to room temperature. To this was added a solution of bis-(dibenzoylmethanato)cobalt(II) (0.039 g, 0.076 mmol) in dry acetonitrile with the resulting solution covered and allowed to stand under ambient conditions. Orange plates, **1a**, suitable for X-ray diffraction appeared after 4 days. Mp >300 °C.

[4-(2-Methylbenzimidazol-1-yl)methylbenzamide]bis-(dibenzoylmethanato)nickel(II) THF, 1b. 1 (0.040 g, 0.153mmol) was dissolved in dry THF with heat in a small vial and cooled to room temperature. To this solution was added bis-(dibenzoylmethanato)nickel(II) (0.039 g, 0.076mmol) dissolved in dry acetonitrile. The resulting solution was covered and allowed to stand under ambient conditions. Green plates, **1b** suitable for X-ray diffraction were obtained after 2 weeks. Mp 283−287 °C (decomp.).

[4-(5,6-Dimethylbenzimidazol-1-yl)methylbenzamide]bis-(hexafluoroacetylacetonato)copper(II), 2a. 2 (0.02 g, 0.0628mmol) and bis-(hexafluoroacetylacetonato)copper(II) (0.01 g, 0.0209mmol) were added to a vial and dissolved with heat in a methanol/acetonitrile mix and allowed to stand under ambient conditions. Green prisms, **2a**, suitable for X-ray diffraction were obtained after a few days. Mp 155−157 °C.

Tetrakis(μ-2-fluorobenzoato-*O*,*O*′)-bis(4-(2-phenylimidazol-1-yl)methylbenzamide)-dicopper(II), 3a. 3 (0.015 g, 0.054 mmol) and Cu(II) 2-fluorobenzoate (0.01 g, 0.018mmol) were added to a beaker and dissolved in acetonitrile. Green prisms, **3a**, suitable for X-ray diffraction were formed after a few days. Mp: 154−157 °C.

Tetrakis(μ-2-fluorobenzoato-*O*,*O*′)-bis(3-(2-phenylimidazol-1-yl)methylbenzamide)-dicopper(II), 4a. 4 (0.015 g, 0.054 mmol) and Cu(II) 2-fluorobenzoate (0.01 g, 0.018mmol) were added to a beaker and dissolved in acetonitrile. Green prisms, **4a**, suitable for X-ray diffraction were formed after 1 h. Mp: 144−146 °C.

[4-(Pyrazol-1-yl)methylbenzamide]bis-(hexafluoroacetylacetonato)copper(II), 5a. 5 (0.025 g, 0.124mmol) and bis-(hexafluoroacetylacetonato)copper(II) (0.03 g, 0.0545mmol) were added to a vial and dissolved with heat in chloroform and allowed to stand under ambient conditions. Green prisms, **5a**, suitable for X-ray diffraction were formed after a few days. Mp 132−135 °C.

[4-(Pyrazol-1-yl)methylbenzamide]bis-(dibenzoylmethanato)nickel(II), 5b. 5 (0.02 g, 0.099mmol) and bis-(dibenzoylmethanato)nickel(II) (0.024 g, 0.0498mmol) were added to a vial and dissolved with heat in ethanol and allowed to stand under ambient conditions. Yellow blocks, **5b**, suitable for X-ray diffraction were formed after a few days. Mp 152−155 °C.

Tetrakis(μ-2-fluorobenzoato-*O*,*O*′)-bis(4-(pyrazol-1-yl)methylbenzamide)-dicopper(II), 5c. 5 (0.015 g, 0.075 mmol) and copper 2-fluorobenzoate (0.0147 g, 0.043 mmol) were added to a beaker and dissolved in acetonitrile. A few drops of acetic acid were added to make the solution transparent, and the solution was allowed to stand under ambient conditions. Aqua-blue prisms, **5c**, suitable for X-ray diffraction were formed after a few days. Mp 208−211 °C.

Tetrakis(μ-acetato-*O*,*O*′)-bis(4-(pyrazol-1-yl)methylbenzamide)-dicopper(II), 5d. 5 (0.015 g, 0.075 mmol) and copper acetate (0.0082 mg, 0.045 mmol) were added to a beaker and dissolved in acetonitrile. A few drops of acetic acid were added to make the solution transparent, and the solution was allowed to stand under ambient conditions. Green prisms, **5d**, suitable for X-ray diffraction were formed after a few days. Mp 149−151 °C.

[3-(Pyrazol-1-yl)methylbenzamide]bis(hexafluoroacetylacetonato)copper(II), 6a. 6 (0.025 g, 0.124mmol) and bis-(hexafluoroacetylacetonato)copper(II) (0.030 g, 0.0545mmol) were added to a vial and dissolved with heat in chloroform and allowed to stand under ambient conditions. Green prisms, **6a**, suitable for X-ray diffraction were formed after a few days. Mp 137−140 °C.

Tetrakis(μ-acetato-*O*,*O*′)-bis(3-(pyrazol-1-yl)methylbenzamide)-dicopper(II), 6b. 6 (0.015 g, 0.082 mmol) and copper acetate (0.0082 g, 0.045 mmol) were added to a beaker and dissolved in acetonitrile. A few drops of acetic acid were added to make the solution transparent, and the solution was allowed to stand under ambient conditions. Green blocks, **6b**, suitable for X-ray diffraction were formed after a few days. Mp 188−190 °C.

X-ray Crystallography. Crystallographic data for all compounds are presented in Table 1.

Results and Discussion

Hydrogen bond geometries for **1a**, **1b**, **2a**, **3a**, **4a**, **5a**−**5d**, and **6a**, **6b** are listed in Table 2.

Compounds **1a** (with Co(II)) and **1b** (with Ni(II)) are isostructural. Both contain two dibenzoylmethanato (dbm) ligands coordinated to a M(II) ion with the remaining axial coordination sites on the metal ion occupied by two 4-[(2-methylbenzimidazol-1-yl)methyl]-benzamide ligands, Co−N, 2.175(2) and (Ni−N, 2.114(4) Å, respectively, resulting in octahedral metal complexes. Neighboring ions are linked by amide···amide hydrogen-bonded dimers involving the *syn*-hydrogen atom and carbonyl oxygen atom (**1a**: N−H···O, 2.954(4) Å), **1b**; (N−H···O, 2.922(6) Å) to generate infinite l-D chains, Figure 1.

Additionally, the *anti*-hydrogen atom of the amide moiety interacts with an oxygen atom of a THF molecule (**1a**: (N−H···O, 2.932(7) Å; **1b**: (N−H···O, 2.975(8) Å). In both structures the intrachain M−M distances is 21 Å.

The crystal structure of **2a** is constructed from two hexafluoroacetylacetonato (hf*acac*) ligands occupying the equatorial sites of the copper(II) ion and the axial sites coordinated by two 4-[(5,6-dimethylbenzimidazol-1-yl)-

Table 1. Crystallographic Data

	1a	1b	2a	5a	5b	6a	3a	4a	5d	5c	6b
formula moiety	$(C_{15}H_{11}O_2)_2Co$ $(C_{16}H_{15}N_3O)_2$ $(C_4H_8O)_2$	$(C_{15}H_{11}O_2)_2Ni$ $(C_{16}H_{15}N_3O)_2$ $(C_4H_8O)_2$	$(C_5H_1F_6O_2)_2Cu$ $(C_{17}H_{17}N_3O)_2$ $(C_2H_3N)_2$	$(C_5H_1F_6O_2)_2Cu$ $(C_{17}H_{17}N_3O)_2$ $(C_2H_3N)_2$	$(C_{15}H_{11}O_2)_2Ni$ $(C_{11}H_{11}N_3O)_2$ $(C_{15}H_{11}O_2)_2$ $(C_2H_6O)_2$ Ni	$(C_5H_1F_6O_2)_4Cu_2$ $(C_{11}H_{11}N_3O)_2$	$(C_7H_4O_2F)_4Cu_2$ $(C_{17}H_{15}N_3O)_2$ $(C_2H_3N)_5$	$(C_7H_4O_2F)_4Cu_2$ $(C_{17}H_{15}N_3O)_2$ $(C_2H_3N)_4$	$(C_2H_3O_2)_4Cu_2$ $(C_{11}H_{11}N_3O)_2$ $(C_2H_3N)_2$	$(C_7H_4O_2F)_4Cu_2$ $(C_{11}H_{11}N_3O)_2$	$(C_2H_3O_2)_4Cu_2$ $(C_{11}H_{11}N_3O_1)_2$
empirical formula	$C_{70}H_{68}CoN_6O_8$	$C_{70}H_{68}N_6NiO_8$	$C_{48}H_{42}CuF_{12}N_8O_6$	$C_{42}H_{26}Cu_2F_{24}N_6O_{10}$	$C_{86}H_{78}N_6Ni_2O_{12}$	$C_{42}H_{26}Cu_2F_{24}N_6O_{10}$	$C_{72}H_{61}Cu_2F_4N_{11}O_{10}$	$C_{70}H_{58}Cu_2F_4N_{10}O_{10}$	$C_{34}H_{40}Cu_2N_8O_{10}$	$C_{50}H_{38}Cu_2F_4N_6O_{10}$	$C_{30}H_{34}Cu_2N_6O_{10}$
molecular weight	1180.23	1180.01	1118.44	1357.77	1504.96	1357.77	1443.40	1402.34	847.82	1085.94	765.71
color, habit	orange plate	green plate	green prism	green prism	yellow block	green prism	green prism	green plate	green prism	blue prism	green block
crystal system	triclinic	triclinic	triclinic	monoclinic	triclinic	monoclinic	triclinic	triclinic	triclinic	monoclinic	triclinic
space group, Z	$P\bar{1}$, 1	$P\bar{1}$, 1	$P\bar{1}$, 1	$P2(1)/c$, 2	$P\bar{1}$, 1	$P2(1)/c$, 2	$P\bar{1}$, 1	$P\bar{1}$, 1	$P\bar{1}$, 1	$P2(1)/c$, 2	$P\bar{1}$, 1
a/Å	8.9670(6)	8.9948(19)	10.349(3)	9.7354(11)	9.0170(6)	10.0325(10)	10.9536(9)	10.9819(16)	7.5896(5)	10.8218(9)	8.0173(4)
b/Å	11.2006(7)	11.185(2)	10.688(3)	11.1497(12)	12.3493(8)	15.1765(15)	11.2155(8)	11.2072(15)	10.0990(7)	19.4000(14)	10.1615(5)
c/Å	15.3238(9)	15.409(3)	12.680(3)	23.870(3)	17.6357(12)	16.6440(16)	14.9765(12)	14.926(2)	13.3959(8)	12.0541(8)	11.4846(6)
α/deg	75.533(3)	75.737(9)	98.217(6)	90	86.3190(10)	90	77.570(6)	99.042(8)	68.531(4)	90	110.1640(10)
β/deg	80.377(4)	79.844(13)	110.457(5)	96.985(2)	78.0890(10)	99.957(2)	78.159(4)	91.419(6)	82.310(3)	108.346(4)	109.1250(10)
γ/deg	79.221(4)	78.971(16)	104.465(5)	90	72.2410(10)	90	74.526(5)	116.183(7)	72.114(3)	90	90.5040(10)
V/Å^3	1452.18(16)	1461.1(5)	1230.8(6)	2571.8(5)	1830.0(2)	2496.0(4)	1710.1(2)	1618.8(4)	909.07(10)	2402.0(3)	821.95(7)
T/K	203(2)	203(2)	100(2)	100(2)	100(2)	100(2)	173(2)	173(2)	173(2)	173(2)	100(2)
ρ/g cm^{-3}	1.350	1.341	1.509	1.753	1.366	1.807	1.402	1.438	1.549	1.501	1.547
X-ray wavelength	0.71073	0.71073	0.71073	0.71073	0.71073	0.71073	0.71073	0.71073	0.71073	0.71073	0.71073
μ/mm^{-1}	0.360	0.397	0.547	0.975	0.584	1.005	0.700	0.737	1.238	0.966	1.359
Θ_{min}/deg	1.38	1.38	2.22	2.02	2.09	2.06	1.41	2.06	1.63	2.07	2.02
Θ_{max}/deg	27.48	27.40	29.95	30.01	30.02	30.11	27.49	27.56	28.28	28.33	30.00
reflections											
collected	10224	9284	13002	24508	21060	28577	12745	12440	14172	17581	9572
independent	6254	6080	6946	7477	10465	7318	7533	7276	4271	5679	4714
observed	4699	3293	5797	6517	8877	6341	5673	5544	3697	4503	4413
threshold expression	>2σ(I)	>2σ(I)	>2σ(I)	>2σ(I)	>2σ(I)	>2σ(I)	>2σ(I)	>2σ(I)	>2σ(I)	>2σ(I)	>2σ(I)
absorption correction	numerical	multiscan	none	multiscan	multiscan	multiscan	multiscan	multiscan	multiscan	none	multiscan
	0.915/0.942	0.481/1.00		0.672/1.00	0.811/1.00	0.784/1.00	0.687/1.00	0.733/1.00	0.763/1.00		0.705/1.00
R_1 (observed)	0.0746	0.0829	0.0653	0.0365	0.0490	0.0356	0.0782	0.0647	0.0529	0.0548	0.0304
wR_2 (all)	0.2109	0.2292	0.1650	0.0972	0.1260	0.0956	0.2236	0.1927	0.1436	0.1467	0.0794

Table 2. Hydrogen Bond Geometries for **1a**, **1b**, **2a**, **3a**, **4a**, **5a**−**5d**, and **6a**, **6b**

compound	D−H···A	D−H/Å	H···A/Å	D···A/Å	<(DHA)/deg	symmetry transformations
1a	N(27)−H(27A)···O(27)#2	0.87	2.09	2.954(4)	171.4	#2 $-x+2,-y,-z$
	N(27)−H(27B)···O(1A)#3	0.87	2.11	2.932(7)	156.8	#3 $-x+2,-y+1,-z$
1b	N(27)−H(27A)···O(27)#2	0.87	2.06	2.922(6)	171.9	#2 $-x+2,-y,-z$
	N(27)−H(27B)···O(1A)#3	0.87	2.17	2.975(8)	153.9	#3 $-x+2,-y+1,-z$
2a	N(37)−H(37B)···N(1S)	0.74(9)	2.41(9)	3.121(9)	163(9)	#1 $-x+1,-y+1,-z+1$
	N(37)−H(37A)···O(37)#2	0.86(9)	2.04(9)	2.896(8)	172(8)	#2 $-x+2,-y,-z$
5a	N(47)−H(47A)···O(24)#1	0.87(2)	2.21(2)	2.9963(19)	150.5(18)	#1 $-x+1,-y+1,-z+1$
	N(47)−H(47B)···O(12)#2	0.82(2)	2.27(2)	3.0105(18)	150(2)	#2 $x-1,y,z$
5b	N(87)−H(87A)···O(41)#3	0.88	2.27	2.943(2)	133.4	#3 $x,y+1,z$
6a	N(47)−H(47A)···O(14)	0.82(2)	2.61(2)	3.2986(19)	143.2(19)	#2 $x,-y+3/2,z-1/2$
	N(47)−H(47B)···O(12)#2	0.85(2)	2.38(2)	3.1466(18)	150.0(19)	
3a	N(37)−H(37B)···N(1S)	0.88	2.19	3.011(7)	154.3	#2 $-x+2,-y+1,-z+1$
	N(37)−H(37A)···O(37)#2	0.88	2.02	2.879(5)	164.4	
4a	N(31)−H(31A)···O(31)#2	0.95(5)	1.91(5)	2.852(5)	169(4)	#2 $-x,-y,-z$
5c	N(27)−H(27A)···O(27)#2	0.88	1.99	2.859(3)	168.8	#2 $-x+1,-y,-z+1$
	N(27)−H(27B)···O(48)#3	0.88	2.43	3.098(3)	132.9	#3 $-x+1/2,y-1/2,-z+1/2$
5d	N(17)−H(17A)···O(31)#2	0.87(4)	2.24(4)	3.086(3)	164(3)	#2 $-x+1,-y+1,-z+1$
	N(17)−H(17B)···N(1S)	0.80(4)	2.26(4)	3.045(4)	167(4)	
6b	N(27)−H(27A)···O(27)#2	0.78(2)	2.16(2)	2.9359(18)	172(2)	#2 $-x,-y+2,-z+1$
	N(27)−H(27B)···O(31)#3	0.81(2)	2.47(2)	3.1634(18)	144(2)	#3 $-x+1,-y+1,-z+1$

methyl]benzamide ligands, (Cu−N, 1.995(5) Å) resulting in an octahedral geometry. The complex is assembled into 1-D chains through amide···amide dimers via N−H···O hydrogen bonds (3.121(9) Å) Figure 2. The *anti*-amide proton forms a hydrogen bond to a MeCN solvent molecule. Copper(II) ions within chains are approximately 22 Å apart.

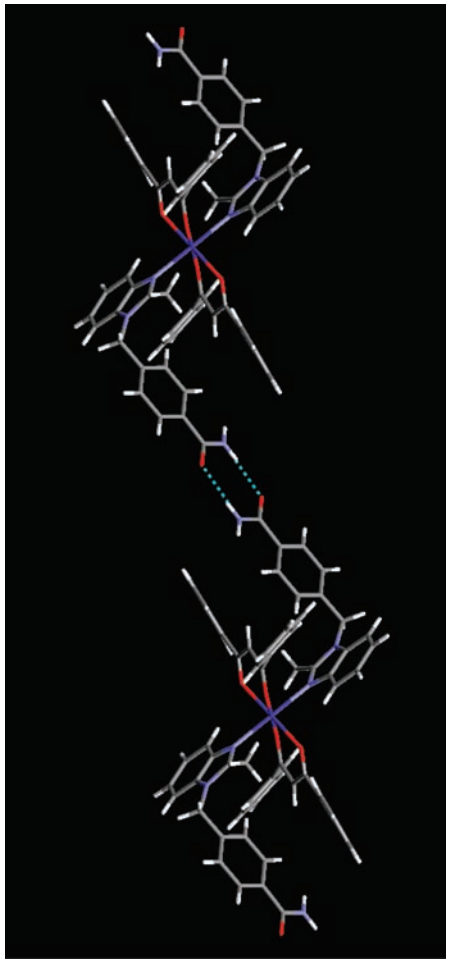

Figure 1. Supramolecular 1-D chain in the structure of **1a**. The Co(II) ions (dark blue) are located in the plane between two chelating dbm ligands (oxygen atoms in red) and coordinated in the axial positions through the nitrogen atoms (light blue) of two benzimidazole ligands. Solvent molecules removed for clarity, and hydrogen bonds shown as blue dotted lines.

The crystal structure of **3a** consists of two 4-[2-phenylimidazol-1-yl)methyl]-benzamide ligands coordinated via the imidazole nitrogen atoms to the axial positions of a copper(II) 2-fluorobenzoate "paddle wheel" unit, Cu−N, 2.162(3) Å, Figure 3.

The metal complex becomes part of an infinite 1-D chain as a result of self-complementary homomeric amide···amide dimers, N−H···O, 2.879(5) Å. Additionally, the *anti*-hydrogen atom of the amide moiety interacts with an acetonitrile molecule via a N−H···N hydrogen bond (3.011(7) Å). The Cu−Cu distance within the "paddle wheel" is 2.6881(9) Å.

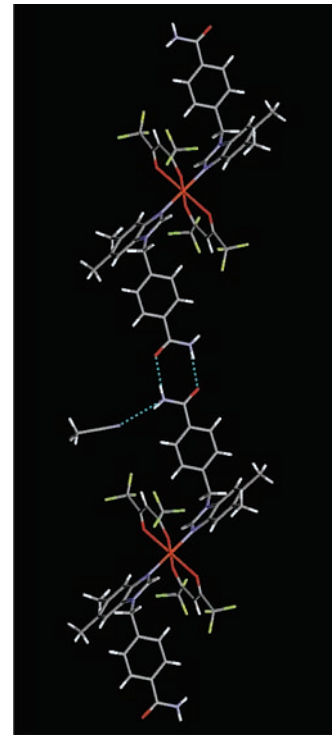

Figure 2. 1-D chain in the crystal structure of **2a**. The Cu(II) ions (orange) are located in the plane between two chelating hf*acac* ligands (oxygen atoms in red, fluorine atoms in yellow) and coordinated in the axial positions through the nitrogen atoms (light blue) of two benzimidazole ligands. Hydrogen bonds shown as blue dotted lines.

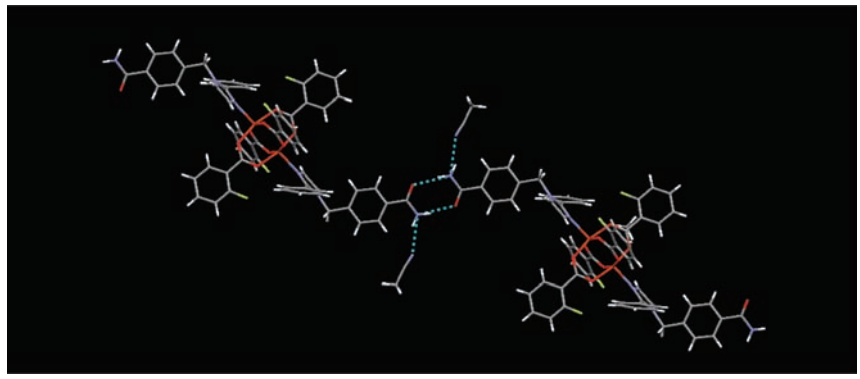

Figure 3. 1-D chain in the crystal structure of **3a**. Each paddlewheel unit comprises two Cu(II) ions (orange) and four benzoate ligands (oxygen atoms in red, fluorine atoms in yellow). The axial positions are occupied by imidazole ligands with coordination through the nitrogen atoms (light blue). Hydrogen bonds shown as blue dotted lines.

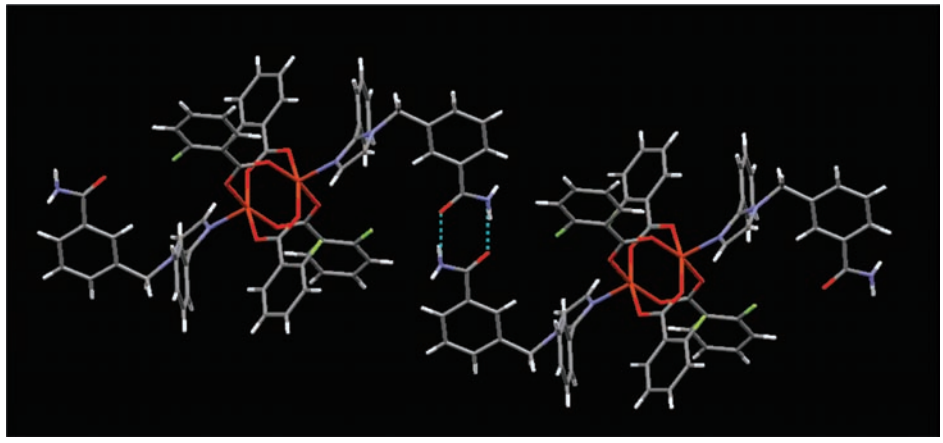

Figure 4. 1-D "wavy" chain in the crystal structure of **4a**. Each paddlewheel unit comprises two Cu(II) ions (orange) and four benzoate ligands (oxygen atoms in red, fluorine atoms in yellow). The axial positions are occupied by imidazole ligands with coordination through the nitrogen atoms (light blue). Hydrogen bonds shown as blue dotted lines.

The crystal structure of **4a** contains two 3-[2-phenylimidazol-1-yl)methyl]-benzamide ligands coordinated to the axial positions of the copper(II) 2-fluorobenzoate "paddle wheel" unit (Cu−N, 2.154(3) Å). 1-D chains are produced through self-complementary amide···amide dimers via N−H···O hydrogen bonds, 2.879(5) Å, Figure. 4. The Cu−Cu distance within the "paddle wheel" is 2.6936(8) Å.

The complex ion in **5c** comprises two 4-[(pyrazol-1-yl)methyl]benzamide ligands coordinated to the axial sites of a copper(II) 2-fluorobenzoate "paddle wheel" unit, Cu−N, 2.165(2) Å, Figure 5.

The ions are subsequently assembled into 1-D chains through amide···amide dimers via N−H···O hydrogen bonds, 2.859(3) Å. The *anti*-hydrogen atom of the amide moiety interacts with a 2-fluorobenzoate oxygen atom via a N−H···O hydrogen bond, 3.098(3) Å. The Cu−Cu distance within the "paddle wheel" unit is 2.6480(5) Å.

The coordination complex, **6b**, consists of two 3-[(pyrazol-1-yl)methyl]benzamide ligands coordinating to the axial positions of a copper(II) acetate "paddle wheel" unit via the pyrazole nitrogen, Cu−N, 2.1908(12) Å, Figure 6. Adjacent complex ions are organized into 1-D chains through amide···amide dimers via N−H···O hydrogen bonds, N···O 2.9359(18) Å. Additionally, the *anti*-hydrogen atom of the amide moiety interacts with an acetate oxygen atom via an N−H···O hydrogen bond, 3.1634(18) Å. The Cu−Cu ions within the "paddle wheel" unit are 2.6596(3) Å apart.

The coordination complex, **5b**, contains two different nickel(II) centers in the unit cell. In one complex, two 4-[(pyrazol-1-yl)methyl]benzamide ligands occupy the axial positions via coordination through the pyrazole nitrogen atoms (Ni−N 2.006(12) Å). However, this time the amide does not engage in a self-complementary dimer but instead forms an O−H···O hydrogen bond (2.733 Å) to an ethanol molecule that is coordinated to the second nickel ion (the second Ni(II) complex has two ethanol molecules in the axial positions and no pyrazole). The *syn*-hydrogen atom of the amide forms a N−H···O hydrogen bond (2.943(2) Å) to an *acac* oxygen atom, Figure 7. The overall primary motif is a 1-D chain (but not assembled in the intended manner) with intrachain Ni−Ni distances of approximately 10.5 Å.

The complex ion in the crystal structure of **5d** contains two 4-[(pyrazol-1-yl)methyl]benzamide ligands coordinated to the free axial sites of a copper(II) acetate "paddle wheel" unit, Cu−N, 2.191(2) Å. This time the intended 1-D chain is disrupted by the presence of an acetonitrile molecule which binds to an amide moiety via a N−H···N hydrogen bond, 3.045(4) Å, and also because the *syn*-hydrogen atom is interacting with an acetate oxygen atom via an N−H···O

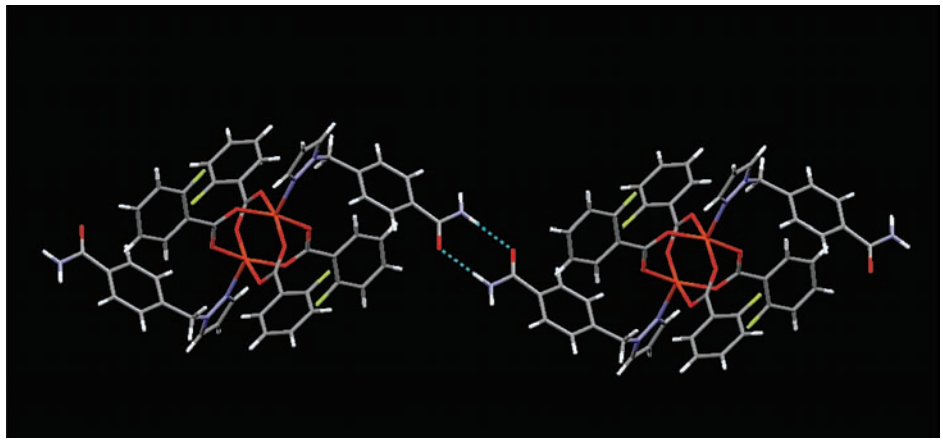

Figure 5. 1-D chain in the crystal structure of **5c**. Each paddlewheel unit comprises two Cu(II) ions (orange) and four benzoate ligands (oxygen atoms in red, fluorine atoms in yellow). The axial positions are occupied by pyrazole ligands with coordination through the nitrogen atoms (light blue). Hydrogen bonds shown as blue dotted lines.

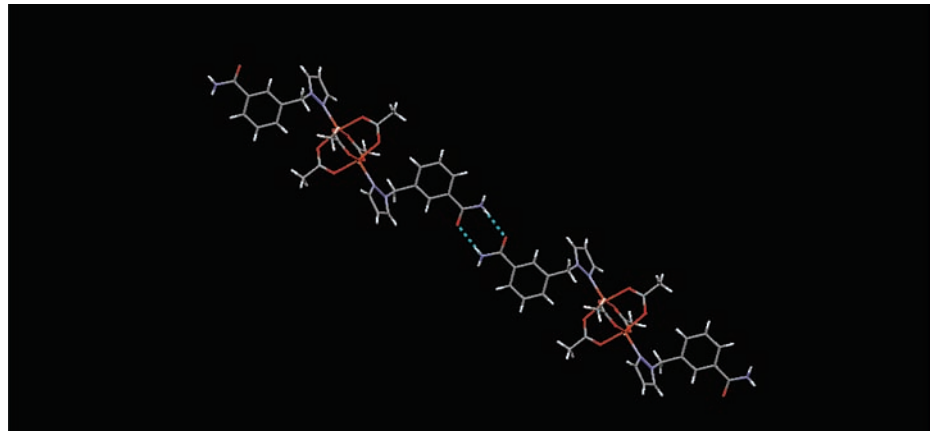

Figure 6. 1-D chain in the crystal structure of **6b**. Each paddlewheel unit comprises two Cu(II) ions (orange) and four acetate ligands (oxygen atoms in red). The axial positions are occupied by pyrazole ligands with coordination through the nitrogen atoms (light blue). Hydrogen bonds shown as blue dotted lines.

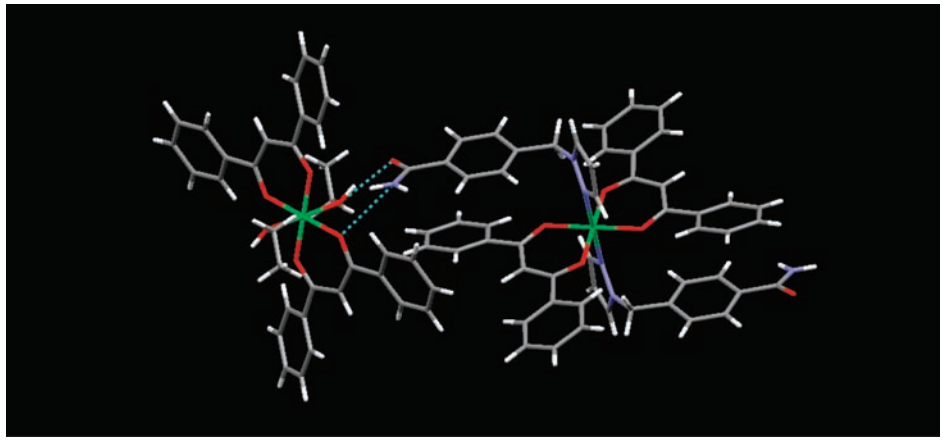

Figure 7. Interaction between the two unique Ni(II) complexes in the crystal structure of **5b**. Ni(II) ions (green) are located in the plane between two chelating *acac* ligands (oxygen atoms in red) and coordinated in the axial positions through (a) the nitrogen atoms (light blue) of two pyrazole ligands and (b) through the oxygen atoms of two ethanol molecules Hydrogen bonds shown as blue dotted lines.

hydrogen bond, 3.086(3) Å, Figure 8. The Cu−Cu distance within the "paddle wheel" unit is 2.6282(5) Å.

The complex ion in the crystal structures of both **5a** and **6a** display unexpected coordination geometries, since the central ions are coordinated to two acac-type ligands in a *cis* arrangement, with the remaining two sites occupied by a pyrazole nitrogen donor, and an amide oxygen donor, Cu−N, 2.0320(13) Å and Cu−O, 2.2297(12) Å, and Cu−N, 2.0040(13) Å and Cu−O, 1.9725(12) Å, respectively. In each compound the result is a discrete metallacyclic species with Cu−Cu distances of approximately 10.3 Å and 9 Å, respectively, Figure. 9. In addition, both *syn* and *anti* amide hydrogen atoms form hydrogen bonds to oxygen atoms of two hf*acac* ligands (N−H···O, 2.9963(19) and 3.0105(18)

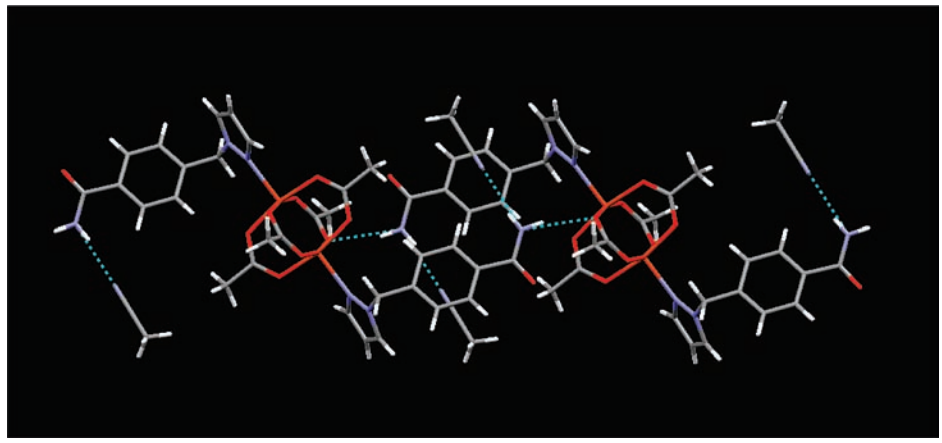

Figure 8. Primary non-covalent interactions in the crystal structure of **5d.** Each paddlewheel unit comprises two Cu(II) ions (orange) and four acetate ligands (oxygen atoms in red). The axial positions are occupied by pyrazole ligands with coordination through the nitrogen atoms (light blue). Hydrogen bonds shown as blue dotted lines.

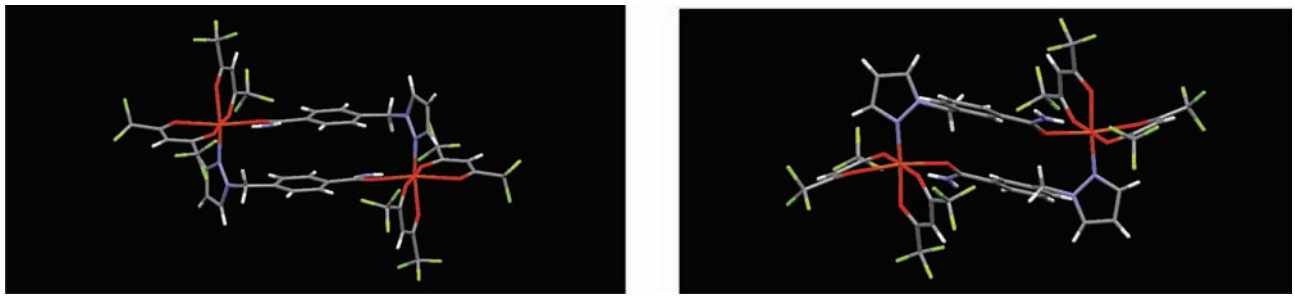

Figure 9. Metallacycles in the crystal structures of **5a** (left), and **6a** (right). Each Cu(II) ion (orange) is coordinated to two chelating hf*acac* ligands (oxygen atoms in red, fluorine atoms in yellow) in a *cis* geometry. The remaining two positions are occupied by pyrazole ligands with coordination through the nitrogen atoms (light blue).

Å, and (N−H···O, 3.2986(19) and 3.1466(18) Å, respectively.

The slight difference in ring size between the metallacycle in **5a** and **6a** is a result of the geometry of the bridging ligand; it is 4-[(pyrazol-1-yl)methyl]benzamide ligands in **5a** whereas it is the 3-isomer in **6a**.

Discussion

The use of chelating *acac* or bridging carboxylate ligands (for generating "paddle wheel" structures) offers an effective method for controlling the coordination chemistry of a variety of first-row transition metals. In nine of the eleven (82%) structures obtained, the desired coordination geometry was obtained, with only **5a** and **6a** failing to produce the intended central metal-containing building block. The subsequent supramolecular synthetic goal, an infinite 1-D chain constructed from amide···amide hydrogen-bond based synthons, was achieved in seven of the remaining nine structures (78%). The high supramolecular yield (i.e., the frequency with which a desired supramolecular motif appears) obtained in this study was supported by existing structural data from the Cambridge Structural Database (CSD).[14] Combining the 11 crystal structures presented herein with the 17 crystal structures containing isonicotinamide and nicotinamide, Table 3, (a search of imidazole and pyrazole amide ligands yielded no hits) gives a supramolecular yield of 86% for the

Table 3. *acac*- and "Paddle-Wheel" Coordination Complexes of Isonicotinamide and Nicotinamide from CSD Search[a]

metal complex	desired metal coordination	amide···amide dimer yielding 1D chain
Isonicotinamide+Co(DBM)$_2$+$CHCl_3$ (HAJPOY)[10a]	√	√
Isonicotinamide+Ni(DBM)$_2$+PhBr (HAJPUE)[10a]	√	√
Isonicotinamide+Co(DBM)$_2$+DMF (HAJQAL)[10a]	√	√
Isonicotinamide+Ni(DBM)$_2$+$CHCl_3$+THF (HAJQEP)[10a]	√	√
Isonicotinamide+Rh$(OAc)_2$+$(CH_3)_2O$ (BEDHEY)[10b]	√	√
Isonicotinamide+Cu$(OAc)_2$+MeCN (EMAWAQ)[10c]	√	√
Isonicotinamide+Cu$(OAc)_2$ (TALKEX)[10d]	√	×
Nicotinamide+Rh$(OAc)_2$+$(CH_3)_2O$ (BEDHIC)[10b]	√	√
Nicotinamide+Cu$(OAc)_2$ (BENQEQ)[10e]	√	√
Nicotinamide+Cu$(OAc)_2$ (BENQAM)[10e]	×	×
Nicotinamide+Cu$(OAc)_2$+H_2O (BEXNOH01)[10f]	√	×
Nicotinamide+Zn$(OAc)_2$+H_2O (TAYFIJ)[10g]	√	×
Nicotinamide+Cu$(OPr)_2$ (VORWUV)[10h]	√	√
Nicotinamide+Cu$(OVal)_2$ (GETQEC)[10i]	√	√
Nicotinamide+Cu$(OHep)_2$ (CAYHIT01)[10j]	√	√
Nicotinamide+Cu$(OHep)_2$ (CAYHIT)[10j]	√	×
Nicotinamide+Cu$(ONon)_2$ (CAYHUF)[10j]	√	×

[a] CSD codes in bold in parentheses.

(14) Cambridge Structural Database, version 5.29, January 2008.

desired coordination chemistry and geometry with a 76% supramolecular yield observed for the formation of an infinite 1-D chain.

It is interesting to note that the effectiveness of the amide moiety to successfully organize adjacent complex ions into infinite chains through amide···amide synthons, approaches the degree of control that can be achieved over the coordination chemistry despite the fact that the former interactions are significantly weaker than most coordinate-covalent bonds.

In the three cases (out of a total of 28 cases) where the desired coordination chemistry was not attained (**5a**, **6a** and **BENQAM**), the amide binds directly to the metal ion via its C═O moiety. It is at this point unclear why both **5a** and **6a** contain a metallacyclic structure. The presence of the hf*acac* ligand in itself does not, based upon existing data and upon structure **2a**, make the Cu(II) predisposed to binding two chelating ligand in a *cis*-manner (which is a prerequisite for a cyclic structure in this context). Furthermore, a particular geometry of the supramolecular ligand is also not, in itself, a noticeable driving force for a cyclic structure. Again, 4-[(5,6-dimethylbenzimidazol-1-yl)methyl]benzamide, which is the supramolecular ligand in **2a**, could readily form a cyclic dinuclear motif but instead it opts for a 1-D chain.

The amide···amide interaction is disrupted in three cases (**5c**, **TALKEX**, and **CAYHIT**) because an oxygen atom from an acetate ligand (as part of the "paddle-wheel" complex) competes successfully for the attention of the *syn*-amide hydrogen atom, which also prevents the formation of a 1-D chain. The fact that the homomeric amide···amide $R_2^2(8)$ motif remains intact 75% of the time even in the presence of ligand-based hydrogen-bond acceptors, serves to underscore its importance as a supramolecular synthetic tool.[11,12] The presence of solvent molecules within the lattice is another potential source of supramolecular strife as many such compounds are very capable hydrogen-bond donors/acceptors. In three cases, **5b**, (ethanol as a ligand), **BEXNOH1**, and **TAYFIJ** (both with non-coordinating H_2O), an included solvent molecule manages to disrupt the amide···amide synthon. For the same reason that hydrogen-bond based supramolecular synthesis is more likely to be successful in the absence of potentially competing counterions, it is also useful to try to avoid solvent molecules such as H_2O, MeOH, and EtOH. In the structures presented in this study, the desired 1-D motif appeared even in the presence of solvents such as chloroform, acetonitrile, DMF, bromobenzene, acetone and THF

Conclusions

Self-complementary hydrogen-bond based amide···amide dimers are shown to be robust supramolecular synthons for the assembly and organization of *acac*- and paddle-wheel complex ions involving a variety of metals. The desired molecular recognition event, and intended extended motif appears with a supramolecular yield of 78% (a total of 28 structures were examined). Despite the fact that the hydrogen bonds that give rise to the $R_2^2(8)$ motif can be disrupted by both carboxylate- and *acac*-ligands, as well as by solvent molecules, they remain remarkable resilient and should therefore be useful as a synthetic tool in a wide range of inorganic crystal engineering efforts. The versatility of the strategy is underscored by the fact that four different N-heterocyclic moieties (imidazole, benzimidazole, pyridine, and pyrazole) have been incorporated into ligands with different geometries, yet the coordinating ability and the supramolecular effectiveness of these bifunctional, structure-directing, compounds have remained consistent.

Acknowledgment. Acknowledgment is made to the Donors of the American Chemical Society Petroleum Research Fund for support (or partial support) of this research (#46011-AC1) and to the NSF (CBET 0609318).

Supporting Information Available: X-ray crystallographic files are available for complexes **1a**, **1b**, **2a**, **3a**, **4a**, **5a**−**5d** and **6a**, **6b**. This material is available free of charge via the Internet at http://pubs.acs.org.

IC801992T